Distinct Mechanical Relaxation Components in Pairs of Erythrocyte Ghosts Undergoing Fusion

Yankuan Wu, Raymond A. Sjodin, and Arthur E. Sowers
Department of Biophysics, School of Medicine, University of Maryland, Baltimore, Maryland 21201 USA

ABSTRACT It was previously reported (Chernomordik and Sowers, 1991) that erythrocyte ghosts which were exposed to a 42°C, 10-min heat treatment would, upon electrofusion, produce over 15–20 s a fusion product with an "open lumen" (i.e., the fusion product became converted to one large sphere), while electrofusion of ghost membranes not so exposed would lead to chains of polyghosts. In phase optics the chains of polyghosts showed a "flat diaphragm" at virtually every ghost-ghost junction (i.e., the ghosts do not appear to be fused even though fluorescent-labeled lipid analogs can laterally diffuse from a labeled ghost to an adjacent unlabeled ghost). In the present study we found that the diameter increase in open lumen- and flat diaphragm-producing fusion processes both had a rapid but short early phase (0–5 s after fusion) which was *exponential* or nearly so and a slow but long late phase (5–120 s after fusion) which was essentially *linear*. Heat treatments at 39 or 42°C caused a minor acceleration in only the late phase, while temperatures of 45 or 50°C caused an immediate and dramatic acceleration in the rate of diameter increase (spheres in 1–2 s). Ghost membranes in the presence of glycerol at 20% (v/v) did not form open lumens when exposed to the 42°C (but not the ≥ 45°C) heat treatment. This suggested that the heat treatment was denaturing a critical protein. Both of these observations are consistent with the involvement of the spectrin network since it is the only protein in the erythrocyte membrane which is known (Brandts et al., 1977) to have a calorimetric transition over the same temperature range used in our heat treatments. The diameter versus time curves were sensitive to: (i) the residual effects of the fusogenic electric pulse only up to about 1 s after the pulse, (ii) the strength of the dielectrophoretic field after the pulse, but not before the pulse, (iii) the ambient temperature during the measurement.

INTRODUCTION

The appearance of a number of membrane fusion pores in a given area shared by two close spaced biomembranes defines a "fusion zone" and has been seen in a number of artificial (Ahkong et al., 1987) and natural contexts (e.g., Knutton, 1977; Pinto da Silva et al., 1980). Using the electrofusion protocol to induce membrane fusion and erythrocyte ghosts as a model, an early paper from this laboratory (Sowers, 1984) described such membrane fusions in terms of lumen-producing and non-lumen-producing fusion products as they were visible by phase optics. Non-lumen-producing fusions (termed in this paper as "flat diaphragm" fusions) always appeared in phase optics as a straight black line at the junction between two ghost membranes in contact. A recent paper from this laboratory (Chernomordik and Sowers, 1991) not only reported that the number of lumen-producing fusions (= "open lumen" fusions) would be dramatically increased if erythrocyte ghosts were subjected to a heat treatment (42°C, 10 m) but also showed that what appeared in phase optics as a flat diaphragm was actually, at the ultrastructure level, a double membrane multiply perforated with fusion pores. Also, because the heat treatment was within the known calorimetric transition for spectrin (Brandts et al., 1977), it was hypothesized (Chernomordik and Sowers, 1991) that the state of spectrin played a significant role in determining the final morphological fate of fusion induced between two plasma membranes.

The purpose of the present study was to: (i) examine the kinetics of the diameter increase in open lumen and flat diaphragm fusion processes with greater spatial and temporal resolution and also over a greater time interval than in the previous work (Chernomordik and Sowers, 1991), (ii) more fully determine the kinetics of fusion zone expansion as a function of heat treatments which involve temperatures that progressively cross the known spectrin calorimetric transition (Brandts et al., 1977), (iii) characterize the effect on these kinetics from the fusogenic electric pulse and the strength of the dielectrophoretic forces which were used to cause membranes to align into the so-called pearl chain formation, and (iv) attempt to make a preliminary qualitative identification of the involved forces. Portions of this work have been reported in preliminary form (Sowers et al., 1993; Wu et al., 1993).

MATERIALS AND METHODS

Membranes

Rabbit erythrocyte ghosts were prepared from rabbit whole blood obtained mixed 1:1 with Alsevers buffer solution from Truslow Farms (Chestertown, MD). The blood-buffer solution (4 ml) was mixed with 25 ml of isotonic sodium phosphate (NaPi) (Dodge et al., 1963) buffer (pH 7.4) and centrifuged at 300 × g for 10 m. The pellet was resuspended with 30 ml of NaPi (5 mM, pH 7.4) and allowed to stand for 20 m and then centrifuged at 10,000 *g* for 20 m. The loose upper two thirds of the whole pellet was transferred to another centrifuge tube and resuspended with NaPi (20 mM, pH 8.5) and centrifuged at 10,000 *g* for 20 m to give a pink pellet. All operations and storage were at 0–4°C unless otherwise noted.

Received for publication 31 August 1993 and in final form 24 September 1993.

Address reprint requests to Dr. Arthur E. Sowers at the Department of Biophysics, School of Medicine, University of Maryland, 455 Howard Hall, 660 West Redwood Street, Baltimore, MD 21201.

© 1994 by the Biophysical Society

0006-3495/94/01/114/06 $2.00

Heat treatment

Ghost membranes in the experimental groups were exposed to a 20-m heat treatment in a water bath at the temperatures as indicated in the figures and with an accuracy of ±0.5°C. Control group membranes received no heat treatment. For glycerination of the membranes, the NaPi buffer was made up to 20 mM strength (pH 8.5) and to the % (v/v) glycerol as given and used to resuspend pelleted ghost membranes immediately after the hemolysis step and in all steps thereafter.

Electrofusion apparatus

The chamber (Abidor and Sowers, 1992) and electric field generating circuitry (Sowers, 1989, 1992) were as previously described, but used with an Olympus OM-2 inverted microscope. To adjust the temperature of the membrane suspension for the assay, liquid nitrogen in a styrofoam box was heated with electrical resistors dissipating enough heat to boil cool gaseous nitrogen into a flexible plastic duct connected to a plastic enclosure surrounding the chamber on the microscope. The temperature was monitored by a digital thermometer which produced readouts updated every 15 s. The temperature in this enclosure was varied by adjusting either the rate of boiling (the cooled gas being warmed from heat entering across the thin plastic duct walls) or, for temperatures above room (20–24°C), the temperature and rate of flow of room air blown into the enclosure with an electric fan after passing across electric resistors dissipating heat at controlled rates.

Image recording

The image produced by the inverted microscope was converted into a video signal with a type TC 651EA CCD camera (Burle Security Products, Lancaster, PA) which then passed through a VTG-22 video timer (FORA, West Newton, MA) to become recorded on videotape with a Panasonic (Secaucus, NJ) AG-1830 VCR.

Fusion zone diameter measurements

Single frames from replayed videotape sequences were captured with a PCVision Plus (Image Technologies Inc., Woburn, MA) frame-grabber in an IBM clone platform. The specimen-to-image magnification was calibrated by using a stage micrometer. Using 400 × magnification from the microscope and 4 × zoom from the JAVA image analysis software, one doublet of erythrocyte ghosts, with each component ghost having an average diameter of 7 μm, occupied 30% of the screen width of the image monitor (640 × 480). The x and y resolution of the position of the cursor on the screen was 0.10 and 0.14 μm per pixel, respectively. Repeated measurements of the position of a detail on the same object yield a reproducibility of less than three pixels in each axis. Time-dependent fusion zone expansions for 7–10 membrane doublets were recorded on videotape for any given variable. Analysis subsequent to recording involved measuring the diameter of one fusion zone at 10 time points over a 120-s expansion period for each pair of fused membranes using the JAVA video analysis software package.

Protocol

Membrane electrofusion was induced as follows in all of the experiments. Normally (see exceptions below), a pre-pulse AC (60 Hz) field strength of $E_{ac,1}$ = 3.25 V/mm (root-mean-square) was used for dielectrophoretic alignment. This field was applied to the erythrocyte ghosts suspension (10^7 membranes/ml) for approximately 60 s to form close membrane contacts through dielectrophoretic alignment and remained on, at the same strength, after the pulse until all measurements were complete (this was done to prevent Brownian motion from disorienting the fused doublets which could obscure accurate measurement of the fusion zone diameter). Only pearl chains containing two ghost members were selected for observation and measurement. After alignment, one exponentially decaying electric pulse ($t_{½}$ = 0.55 ms) was delivered to the membrane suspension through the electrodes in the fusion chamber to produce a peak field strength of E_p = 600 V/mm in the chamber. In some experiments E_p and $t_{½}$ were varied. The AC field after the pulse ($E_{ac,2}$) was kept on for another 3 min to keep the membranes aligned so that the plane of the fusion zone was held parallel to the optic axis while being recorded on videotape. In experiments to determine the effects of different dielectrophoretic field strengths, the prepulse and post pulse dielectrophoresis-inducing field strengths were different.

RESULTS AND DISCUSSION

Overview

Frame-to-frame playback of video sequences showed that fusion of ghost doublets always occurred via one of two pathways. In the first pathway, the membrane area in the contact zone (the shared membrane area before fusion) became a "fusion zone" (FZ) which remained visible in phase optics as a black line throughout the 120-s observation period while becoming extended in length (Fig. 1, *inset*, *A*). This fusion zone will be referred to as the "flat diaphragm"-type fusion zone. In the second pathway, the flat diaphragm appeared to "dissolve" in a gradual fashion, taking many seconds to become invisible, but doing so at some time substantially before the end of the 120-s observation period (Fig. 1, *inset*, *B*). Products of the second fusion pathway will be referred to as having an "open lumen" FZ. Thus, every fusion causes a flat diaphragm to be produced which can be either stable (i.e., be permanent) or unstable (i.e., having a lifetime which is distinct and finitely shorter than the observation period).

Detection of kinetic phases

Fig. 1 is the FZ diameter versus time relationship plotted on a single linear scale for 42°C, 20-m heat-treated and control membranes and for three fusogenic electric pulse field strengths. Because there was extensive overlap and crowding in the 0–5-s interval and much overlap in the 5–120-s interval, all data were plotted offset relative to each other (absolute values for the diameter at any time can be derived by use of the vertical scale bar and the terminal FZ diameters as given in the figure at 120 s). Since diameter measurements made at 1-s intervals more than 5 s after fusion *appeared*, within experimental error, to *always* be on a straight or essentially straight line, we discontinued making diameter measurements every 1 s as a routine part of the protocol and, for clarity and consistency, omitted plotting those data points which we did have. Fig. 1 thus revealed a two phase curve: an obvious nonlinear and rapid expansion in the first 5 s followed by an apparent linear and slow expansion in the following 5–120-s interval. Because data points in the 0–5-s period were so close to each other, subsequent plots (e.g., Fig. 1, *inset*) were made on a double scale x axis with an expanded scale for data from the 0–5-s interval and a compressed scale for the data from the 30–120-s subinterval of the entire 5–120-s interval. Data from the 5–30-s segment were deliberately omitted since: (i) their position on the same straight line as the 30–120-s data suggested that no specific kinetic details would be otherwise lost and (ii) to accentuate

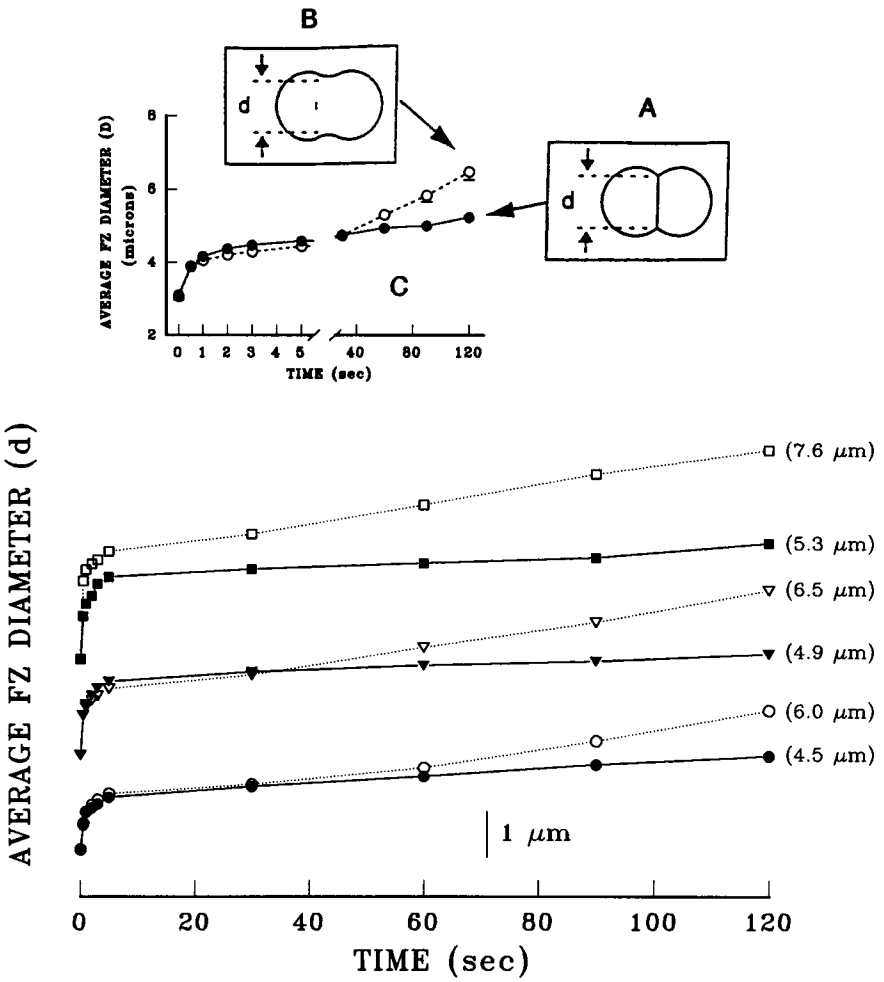

FIGURE 1 Linear-linear but parallel offset (for clarity) plots of average (N = 7) diameter versus time relationships in fused pairs of erythrocyte ghosts with a single time scale on the x axis for: control (*solid symbols*) or heat-treated (*open symbols*) membranes fused with a single 400 V/mm (○, ●), 600 V/mm (▽, ▼), or 800 V/mm (□, ■) electric pulse with a decay half-time of 0.95 ms ($E_{ac,1}$ = $E_{ac,2}$ = 3.25 V/mm). Vertical scale bar is 1.0 μm and FZ diameters (in μm) at 120 s are given in parentheses. All membranes in 20 mM NaPi (pH 8.5) at 20–22°C at time of assay. *Insets A* and *B*: flat diaphragm FZ as obtained from control membranes, and open lumen FZ as obtained from membranes exposed to a 42°C, 20-min heat treatment, respectively (see text). *Inset C*: plots on double scale x axis (see text) and are for flat diaphragm (●) and open lumen (○) fusion zone diameters versus time. Conditions same as in linear-linear plot except that fusion induced with single D.C. electric pulse (E_{dc} = 600 V/mm, decay half-time = 0.55 ms).

the fact that the x-axis scales are different. It should be understood that because of this manner of plotting, the slopes on the right half appear higher than the left half but in fact the absolute rates are (numerically) actually lower. The usefulness of the double scale x-axis plots is that it facilitates the detection of effects from a given experimental condition on processes occurring in the 0–5 versus the 5–120-s intervals (see figures below).

Further examination of data from the 0–5-s interval in Fig. 1, *inset*, shows that the fusion zone diameter at first expanded with maximum velocity at the beginning of the 0–1-s interval, but then decelerated by the end of the 0–1-s interval into an apparently constant or near constant rate upon entry into the 1–5-s interval. Most of the other diameter versus time curves (see Figs. 3-6) also appeared flat or relatively flat over the 1–5-s interval. However, when *rates* ($\Delta d/\Delta t$) of diameter increase versus time were calculated from all of the data in Fig. 1, and plotted as a function of time, as shown in Fig. 2, the rates of change continuously decreased monotonicly over the 0–5-s interval (i.e., the rates in the 1–5-s interval were actually not constant). Also, there was no significant difference between control and 42°C, 20-min heat-treated ghost membranes over the 0–5-s interval. Rate data for the 5–120-s interval showed that for the control membranes the diameter expansion rate appeared to continue its decrease to a still slower rate, ending at about 0.01 μm/s around 10–20 s after the pulse, where it appeared to begin to significantly diverge from the curve for the 42°C, 20-m heat treated ghost membranes (Fig. 2). From that time on, the rate of fusion zone expansion remained at about 0.015–0.02 μm/s, and appeared to be nearly constant, for the heat-treated ghosts. The rate for the control ghosts stayed at about 0.005 μm/s, especially in the 40–120-s subinterval.

It would appear that future work should include more diameter versus time data from the 5–20-s interval after the pulse. Furthermore, quantitative analytical work will necessitate that appropriate attention be directed at criteria that establish qualitative characteristics before data are compared to models.

Effect of the temperature (39, 42, 45, or 50°C) of the heat treatment (Fig. 3) on the diameter versus time curves

For a 39°C heat treatment, the fusion zone diameter in the 5–120-s interval was higher at all times after the pulse than for no heat treatment (i.e., control) but a little lower than for the 42°C heat treatment. The slopes of curves were, however,

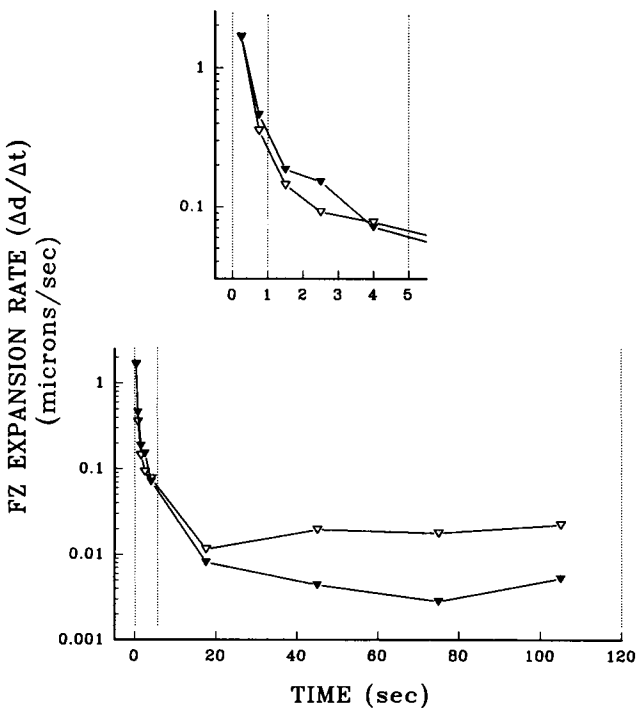

FIGURE 2 Average rates ($\Delta d/\Delta t$) of diameter increase versus time in fusion zones of control (▼), and 42°C, 20-m heat-treated (▽) ghost membranes fused with a single 600 V/mm, 0.55-ms decay half-time electric field pulse (▽ and ▼ data from Fig. 1). *Inset*: rates over the 0–5-s interval.

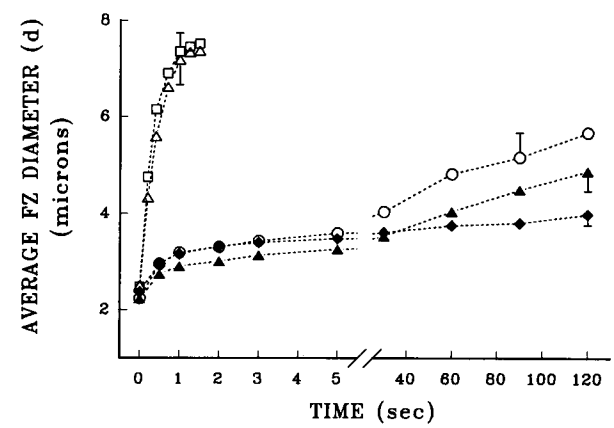

FIGURE 3 Average time-dependent increases in a population of open lumen fusion zones induced between pairs of erythrocyte ghosts held in contact with $E_{ac,1} = E_{ac,2} = 3.25$ V/mm. Other conditions and error bars were as given in Fig. 2, except that the membranes were subject to a 20-min heat treatment at ▲, 39; ○, 42; □, 45; or △, 50°C prior to the assay of fusion zone diameter increase (◆, control = no heat treatment). Control and 39°C heat treatment membranes show only flat diaphragm fusion zones. Bars are standard deviations.

similar. A heat treatment at either 45 or 50°C caused the fusion zone diameter to increase at a dramatically higher rate than at lower temperatures; in both cases a completely spherical fusion product formed by the end of the early phase.

It has been rigorously established that an irreversible calorimetric transition takes place over the 35–50°C range in erythrocyte membranes which is specifically associated with spectrin (Brandts et al., 1977). Spectrin-free membranes show very minor heat absorptions compared to spectrin-bearing membranes, and the isolated spectrin undergoes a calorimetric transition which is similar to that when it is bound to the membrane. The fact that there is substantial overlap between this calorimetric transition temperature range and the temperature range over which there is a concomitant and irreversible change in the normal fusion zone *d* versus time kinetics is additional evidence that we may be observing a spectrin specific or spectrin-associated effect. It is acknowledged that heat treatments, which can induce a loss of plasma membrane area by a still poorly understood vesiculation process (Beaudoin and Grondin, 1991), might also lead to, for example, a differential loss of lipid from the two membrane leaflets thus generating a new membrane bending moment (Evans, 1974). It remains for future experiments to determine whether this possible mechanism could make significant contributions to the observed effects.

Further characterization of the diameter versus time kinetics

The time dependence of the expansion of the fusion zone diameter, *d*, in 42°C, 20-m heat-treated membranes was also examined as a function of: (i) DC pulse field strength, (ii) prepulse and post-pulse AC field strength, (iii) ambient temperature *during the assay*, and (iv) glycerol concentration. The reasons, respectively, for these characterizations are as follows. While higher fusogenic pulse field strengths or pulse durations lead to higher fusion yields (Sowers, 1989, 1992), it cannot be predicted whether the pulse filed strength affects all or just part of the fusion zone diameter versus time curves. The dielectrophortic force which draws the ghost membranes into contact via the so-called "pearl chain formation" is also known to cause a membrane deformation (Dimitrov et al., 1990) but only measurements can determine if a change in this force before or after the pulse could influence the fusion zone diameter versus time curves. It has been established that membrane fluidity is highly temperature-dependent (Kimmelberg, 1979) over temperature ranges likely to be encountered by a biomembrane but surface tension, expected to be a force in cell rounding (Harvey, 1954) is not expected to be strongly temperature-dependent. Thus, the effect of temperature on diameter versus time measurements is expected to provide a clue from this variable. Lastly, glycerol is a convenient and nontoxic method of increasing aqueous viscosity, elevating protein denaturation temperatures (Manning et al., 1989), and dehydrating membranes.

The field strength (Fig. 1) and pulse duration (data not shown) of the fusogenic electric pulse caused an increase in the rate of fusion zone diameter but only in the first 0–1 s after the pulse. All diameter versus time curves within the control and 42°C, heat-treated groups appear to be parallel to each other thereafter. This indicates that the relaxation process may be independent of pulse-induced but long-lived membrane changes such as may occur with electropore induction.

The expansion *rates* of the open lumen fusion zones were in proportion to the ambient temperature (during the measurements) throughout the measurement period (Fig. 4) which is consistent with the expectation that membrane viscosity should be a factor controlling the observed process.

The expansion rates of the open lumen fusion zones were highly dependent on the strength of the dielectrophoretic field in the late phase (5–120 s) and much less so in the early phase (0–5 s) of the diameter versus time curves for the AC field *after* the pulse (Fig. 5) but these rates were not dependent on it at all *before* the pulse (data not shown but all curves were essentially identical to the ○ symbol in Fig. 5). It can be concluded that the dielectrophoretic force generated by the AC field causes a mild but effective force to develop in the fusion zone which is in the same direction as the force which causes the fusion zone diameter to increase anyway. This conclusion is consistent with a previous study (Dimitrov et al., 1990) in which the contact zone diameter was found to be in proportion to the strength of the AC field suggesting that at least the membrane area in the contact zone is under dielectrophoretically induced tension. This finding suggests that the analysis of the AC field induced forces which influence the expansion of fusion zone may permit a new biomechanics technique to be developed.

The presence of glycerol (5 or 20%) during *both* the heat treatment (42°C, 20 m) and the measurement (at 20°C) of the FZ diameter versus time relationship: (*a*) prevented open lumen-type FZs from forming, and (*b*) caused a large lowering of the rate of increase in the early phase (0–5 s) and a smaller lowering in the late phase (5–120 s) in proportion to the concentration of glycerol (Fig. 6). However, these two effects were overcome if the heat treatment reached 45 and 50°C: the fusion zone diameters expanded to their full limits within about 1–2 s as if glycerol were not present at all (data not shown but identical to open squares and open triangles in Fig. 3). This may have been due to the known effects of, for example, polyalcohols (Manning et al., 1989) and salts (Ralston and Dunbar, 1979) which protect proteins from thermal denaturation by elevating their transition temperatures. Thus glycerol, in the first case, protected spectrin from being denatured at 42°C, but could not protect against the effect of the heat treatment when carried out at 45°C, a higher temperature.

The experiments with glycerol allow additional conclusions to be made as follows. As soon as the process of membrane fusion of the two erythrocyte ghosts is completed, the total fused membrane area will be both defined and constant, but the total volume enclosed by the fusion product membrane will increase with time as the fusion zone diameter increases. In other words, the fused doublet will increase in

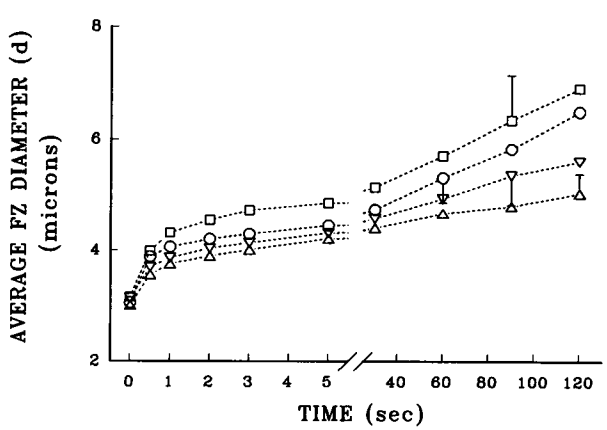

FIGURE 4 Average time-dependent diameter increases in a population of open lumen fusion zones induced between pairs of erythrocyte ghosts held in contact by dielectrophoresis with $E_{ac,1} = E_{ac,2} = 3.25$ V/mm. Other conditions were as given in Fig. 1, except that the ambient temperature of the chamber and its contents were allowed to thermally equilibrate to and stay at: △, 4–6; ▽, 10–12; ○, 20–22; and □, 32–33°C throughout the assay. All other conditions and error bars were as given in Fig. 3.

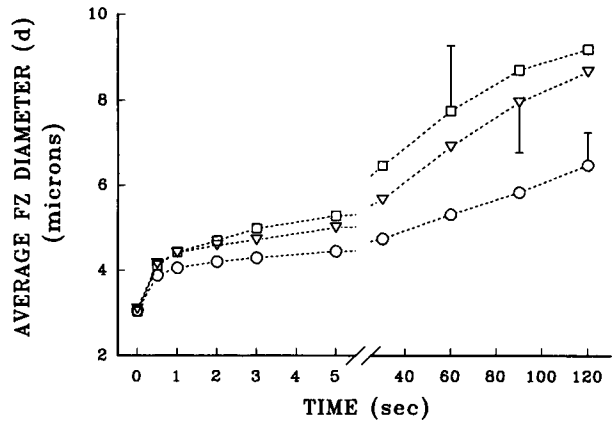

FIGURE 5 Average time-dependent diameter increases for a population of open lumen fusion zones induced between pairs of erythrocyte ghosts held in contact by dielectrophoresis with a prepulse dielectrophoresis AC (60 Hz, sine wave) field strength of ($E_{ac,1}$ = 3.25 V/mm) and post pulse dielectrophoresis field strengths of ($E_{ac,2}$ = ○, 3.25; ▽, 4.25; □, 5.25 V/mm). Error bars are representative standard deviations. Other conditions were as in Fig. 1, *inset C*.

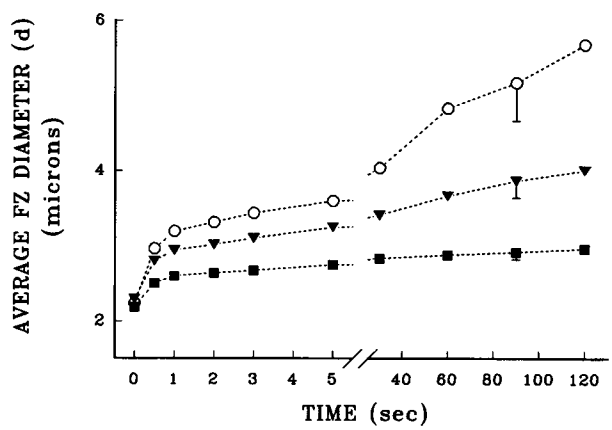

FIGURE 6 Average time-dependent diameter increases in a population of fusion zones induced between pairs of heat treated (42°C, 20 min) erythrocyte ghosts in presence of glycerol (only during the diameter versus time assay) at 5% (▼) and 20% glycerol (■), v/v, compared to control (○). Note: both glycerol treatments led to flat diaphragm fusion zones. Other conditions and error bars were as given in Fig. 3.

volume as it attempts to form one large sphere. Thus it is possible that the passive aqueous permeability of the membrane, the viscosity of the buffer solution, or the physical viscoelasticity of the membrane itself could restrain the increase in the diameter of the fusion zone. It can be concluded, however, that since the fastest fusion zone diameter increases were identical for 45°C and 50°C heat treatments, even if 20% glycerol were present, then neither the viscosity of the medium nor the permeability of the membranes nor the level of hydration at the membrane-solution interface could have contributed a significant force to restrain the increase in FZ diameter.

Our results have implications for three fundamental but interrelated areas of interest. First, numerous past studies (DeBruijne and Steveninck, 1979; Heath et al., 1982; Mohandes et al., 1978; and Rakow and Hochmuth, 1975), using a variety of techniques on erythrocyte membranes, universally report that heat treatments result in a *reduction* in deformability. However, our results show such heat treatments to *increase* "deformability," at least in terms of the rapid rate at which the fusion zone expands. This apparent discrepancy invites future analysis that will surely improve our understanding of the mechanisms underlying membrane and cell deformability. Second, it might be intuitively obvious that the presence of flat diaphragm fusion zones in control membranes physically restrains the FZ diameter from increasing as fast in the 5–120-s interval compared to the situation where $\geq$ 42°C heat treatments cause this flat diaphragm to break down and show higher rates of diameter increase. However, this is not the case since frame-to-frame inspection of individual fusions in the "linear" portion (i.e., the 5–120-s period) of the diameter versus time data showed flat diaphragm lifetimes ranging from as short as 1 s to as long as 60–90 s. In most individual cases the diameter versus time curves appeared to be linear both before and after the diaphragm "dissolved" thus indicating that the flat diaphragm must be easily stretchable compared to the forces which cause the stretching. These forces must therefore originate from outside of the fusion zone. Third, in contrast to the observable effect of a 42°C heat treatment on the diameter versus time kinetic rates in the late phase of fusion zone the rate increase is relatively small compared to the effect of a heat treatment which reaches 45°C. As shown above, hydration, permeability, and membrane viscosity are unlikely to contribute restraining forces to prevent the formation of a sphere in 1–2 s. Thus, over the 42–45°C range, a global and cooperative conformational change takes place which leads to a dramatic change in its properties which control the post-fusion rounding up process and that the element which may be responsible for this is the spectrin network.

Supported by ONR grant N00014-92-J-1053 (to A. E. Sowers) and National Science Foundation grant DCB-8916284 (to R. A. Sjodin).

REFERENCES

Abidor, I. G., and A. E. Sowers. 1992. Kinetics and mechanism of cell membrane electrofusion. *Biophys. J.* 61:1557–1563.

Ahkong, Q. F., J.-P. Desmazes, D. Georgescauld, and J. A. Lucy. 1987. Movements of fluorescent probes in the mechanism of cell fusion induced by poly(ethylene) glycol. *J. Cell Sci.* 88:389–398.

Beaudoin, A. R., and G. Grondin. 1991. Shedding of vesicular material from the cell surface of eukaryotic cells: different cellular phenomena. *Biochim. Biophys. Acta.* 1071:203–219.

Brandts, J. F., L. Erickson, K. Lysko, A. T. Schwartz, and R. D. Taverna. 1977. Calorimetric studies of the structural transitions of the human erythrocyte membrane. The involvement of spectrin in the A transition. *Biochemistry.* 16:3450–3454.

Chernomordik, L. V., and A. E. Sowers. 1991. Evidence that the spectrin network and a nonosmotic force control the fusion product morphology in electrofused erythrocyte ghosts. *Biophys. J.* 60:1026–1037.

DeBruijne, A. W., and J. Van Steveninck. 1979. The effect of anesthetics and heat treatment on deformability and osmotic fragility of red blood cells. *Biochem. Pharmacol.* 28:177–182.

Dimitrov, D. S., M. A. Apostelova, and A. E. Sowers. 1990. Attraction, deformation and contact of membranes induced by low frequency electric fields. *Biochim. Biophys. Acta.* 1023:389–397.

Dodge, J. T., C. Mitchell, D. J. Hanahan. 1963. The preparation and chemical characteristics of hemoglobin-free ghosts of human erythrocytes. *Arch. Biochem. Biophys.* 100:119–130.

Evans, E. A. 1974. Bending resistance and chemically induced moments in membrane bilayers. *Biophys. J.* 14:923–931.

Harvey, E. N. 1954. Tension at the cell surface. *Protoplasmatologia.* 2:1–30.

Heath, B. P., N. Mohandas, J. L. Wyatt, and S. B. Shohet. 1982. Deformability of isolated red blood cell membranes. *Biochim. Biophys. Acta.* 943:411–418.

Kimmelberg, H. K. 1977. The influence of membrane fluidity on the activity of membrane-bound enzymes. *In* Dynamic Aspects of Cell Surface Organization. G. Poste and G. Nicolson, editors. Elsevier/North Holland Biomedical Press. 205–293.

Knutton, S. 1977. Studies of membrane fusion. II. fusion of human erythrocytes by sendai virus. *J. Cell Sci.* 28:189–210.

Manning, M. C., K. Patel, and R. T. Borchardt. 1989. Stability of protein pharmaceuticals. *Pharmaceut. Res.* 6:903–918.

Mohandas, N., A. C. Greenquist, and S. B. Shohet. 1978. Effects of heat and metabolic depletion on erythrocyte deformability, spectrin extractability and phosphorylation. *In* The Red Cell. G. J. Brewer, editor. Alan R. Liss, Inc., New York. 453–472.

Pinto da Silva, P., K. Shimizu, and C. Parkison. 1980. Fusion of human erythrocytes induced by sendai virus: freeze-fracture aspects. *J. Cell Sci.* 43:419–432.

Rakow, A. L., and R. M. Hochmuth. 1975. Effects of heat treatment on the elasticity of human erythrocyte membrane. *Biophys. J.* 15:1095–1100.

Ralston, G. B., and J. C. Dunbar. 1979. Salt and temperature-dependent conformation changes in spectrin from human erythrocyte membranes. *Biochim. Biophys. Acta.* 579:20–30.

Sowers, A. E. 1984. Characterization of Electric Field-Induced Fusion in Erythrocyte Ghost Membranes. *J. Cell Biol.* 99:1989–1996.

Sowers, A. E. 1989. The Mechanism of Electroporation and Electrofusion in Erythrocyte Membranes. *In* Electroporation and Electrofusion in Cell Biology. E. Neumann, A. E. Sowers, and C. Jordan, editors. Plenum Press, New York. 229–256.

Sowers, A. E. 1992. Mechanisms of Electroporation and Electrofusion. *In* Guide to Electroporation and Electrofusion. D. C. Chang, B. M. Chassy, J. A. Saunders, and A. E. Sowers, editors. Academic Press, San Diego. 119–138.

Sowers, A. E., Y. Wu, G. K. Lewis, and R. A. Sjodin. 1993. Multiple, spectrin-related but independent mechanical relaxation components in erythrocyte ghosts undergoing fusion. *Biophys. J.* 64:307*a*. (Abstr.)

Wu, Y., R. A. Sjodin, K. Foster, and A. E. Sowers. 1993. What happens to a fusion zone after fusion pores are created in it? *Biophys. J.* 64:190*a*. (Abstr.)